

CHROM. 22 921

Simultaneous conductivity and potentiometric detector for miniaturized liquid chromatography and flow analysis

K. ŠLAIS

Institute of Analytical Chemistry, Czechoslovak Academy of Sciences, Veveří 97, CS-611 42 Brno (Czechoslovakia)

(First received June 28th, 1990; revised manuscript received October 16th, 1990)

ABSTRACT

A miniature three-electrode electrochemical flow cell with a measuring volume of 0.15 μl together with appropriate electronics was designed to provide simultaneous potentiometric and conductivity measurements of flowing liquids. An antimony working electrode in the cell was used for potentiometric pH monitoring. The suitability of the detector for miniaturized flow-injection analysis and microcolumn liquid chromatography and the mutual independence of both signals obtained was demonstrated. The detector is capable of detecting changes of 50 nS cm^{-1} in conductivity and 0.004 in pH.

INTRODUCTION

Liquid chromatography (LC) is an important method for the separation of ionized compounds. The control of pH and ionic strength of the mobile phase are the main factors for the optimization of the separation of sample components [1–3]. In using standard LC equipment and methods, the pH is usually adjusted by varying the composition of the mobile phase prior to its entering the separation column. When using some form of internal gradient of pH (*i.e.*, chromatofocusing [4]), the actual pH profile during the analysis can be monitored only by measurement of the column effluent. When developing methods with internal gradients [5–8], the pH profile was determined almost exclusively by inconvenient measurement of the collected fractions. Further, when using microcolumns [9,10], the actual pH profile was not known.

Continuous on-line monitoring of pH was developed mainly for flow-injection analysis (FIA) [11]. The widely used flow-through glass electrode has also been modified for the measurement of column effluents in LC [12,13]. However, such devices have a cell volume that is too large to combine effectively with microcolumn LC. It was reported earlier [14,15] that the pH of the column effluent can be monitored also by electrochemical detection. However, the nature of this phenomenon is still to be explained.

In addition to the glass electrode, the antimony electrode has been used for pH measurements in the past. The disadvantages of the antimony electrode are its lower precision and sensitivity towards some complexing organic anions, but it offers some

advantages with regard to miniaturization. It has a low electrical resistance and it is possible to measure pH in sub-microlitre volumes [16,17].

The post-column monitoring of ionic strength is important mainly if the ionic strength changes owing to the internal gradient on the microcolumn [18]. The actual ionic strength is conveniently measured by determination of effluent conductivity (κ).

As both ionic strength and pH are important for the separation of ionic compounds by LC [1–3], the simultaneous measurement of pH and conductivity is advantageous for the development and reproducibility of gradient analysis. The simultaneous measurement of pH and conductivity can be also useful for the study of the nature of the isocratic separation of ionic compounds, as both pH and conductivity change within the zone of an eluted solute [15,19].

The introduction of miniaturized versions of liquid chromatography (micro-LC) places strong demands on the detector cell volume and connections. Simultaneous detection can be achieved most effectively with detectors that offer more than one independent signal from the single miniature flow cell. Further, the evaluation of the signals obtained is not complicated by time and volume shifts.

In this paper, a simultaneous pH and conductivity detector with a three-electrode miniature flow cell with an antimony working microelectrode is described. The electronics of the detector are based on a modified simultaneous conductivity and amperometric detector [20]. The detector was tested under the conditions of miniaturized FIA and micro-LC of small ions.

EXPERIMENTAL

Cell design

The scheme of the cell is shown in Fig. 1. When developing this cell, several important aspects were taken into consideration. First, the reference electrode was placed downstream of the working electrode in order to avoid influencing the latter by the reference electrode electrolyte. Second, in order to maintain the long-term stability of the reference electrode, the loss of the reference electrode electrolyte should be minimized, as it leads to a relatively large electrical resistance of the salt bridge to the measured solution. It does not disturb the pH measurement, but it affects the upper limit of the linearity of the conductivity measurement. Therefore, a three-electrode configuration of the measuring cell was adopted. Third, it is difficult to avoid completely contact of the reference electrode electrolyte with the working electrode, *e.g.*, with the cell out of operation. As the performance of an antimony electrode is sensitive to the presence of noble metal ions in the measured liquid [17,21], the use of mercury- or silver-based reference electrodes was avoided. The lead/lead sulphate electrode in saturated ammonium sulphate solution provided acceptable long-term stability of the pH signal.

The cell constant ($150 \pm 2 \text{ cm}^{-1}$) was determined by calibrating with 0.1 mol l^{-1} potassium chloride solution. The volume between the working and auxiliary electrodes was calculated to be 150 nl.

The equivalent electric circuitry of the cell is shown in Fig. 1B. The working, reference and auxiliary electrodes (*w*, *r* and *a* respectively) can be characterized by their potential vs. liquid (E_w , E_r , E_a), the double layer capacitance (C_w , C_r , C_a) and Faradaic impedance (Z_w , Z_r , Z_a). The measured electrolyte represents the resistance R_e and R_r is

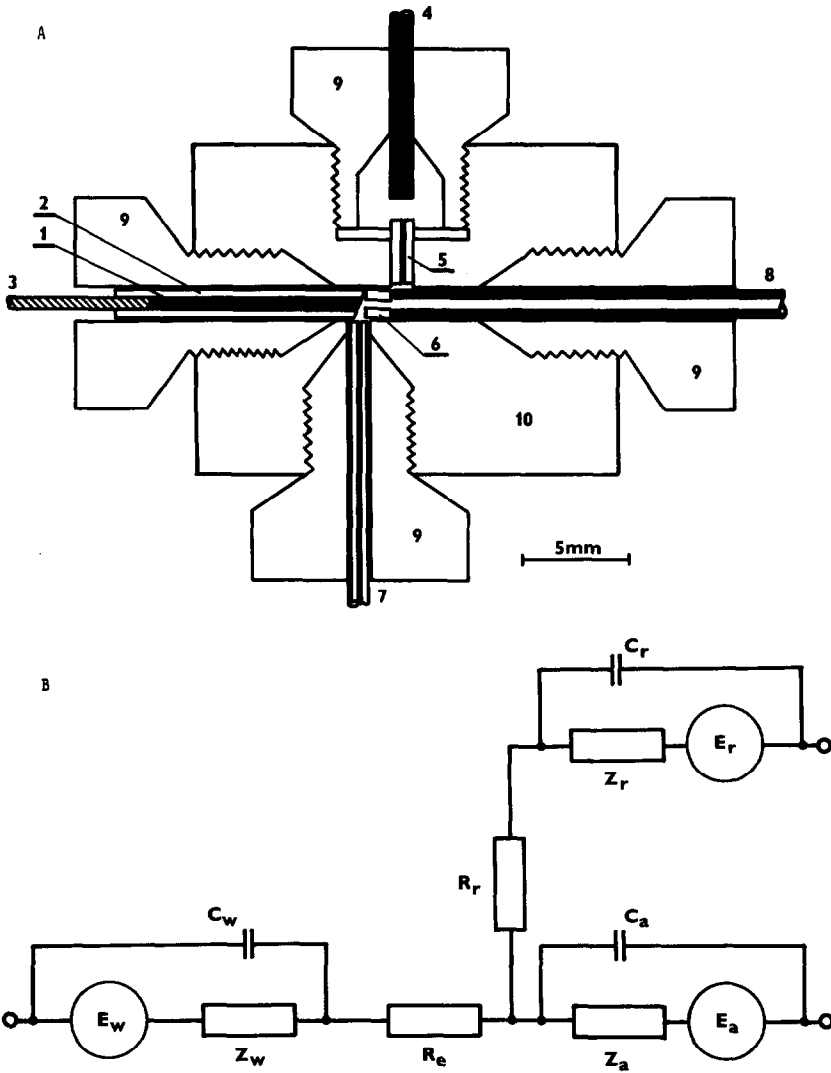


Fig. 1. (A) Flow cell. 1 = Antimony working microelectrode; 2 = glass capillary jacket of working electrode; 3 = copper contact to working electrode; 4 = lead reference electrode; 5 = glass capillary bridge to reference electrode; 6 = glass capillary; 7 = Teflon inlet capillary; 8 = stainless-steel outlet capillary used as an auxiliary electrode; 9 = plastic screw; 10 = acrylate cell body. (B) Equivalent electric circuitry of the cell. E = Sources of voltage; Z = Faradaic impedances; C = double-layer capacitances; subscripts w, r and a represent working, reference and auxiliary electrodes, respectively; R_e = flow cell electrolyte resistance; R_r = resistance of salt bridge between flow cell and reference electrode.

the resistance of the salt bridge between the reference electrode and the measured liquid.

The measurement of pH is based on sensing of the direct potential difference between the working and reference electrodes in the absence of direct current between

these electrodes. Then all resistances, impedances and capacitances of the cell do not interfere.

The measurement of the solution conductivity is based on the determination of R_e . The influence of E and Z is avoided by applying an a.c. voltage of sufficiently high frequency. For the resulting alternating current, the impedances of C are then substantially lower than those of R_e and Z . However, the influence of R_r is not removed in this way. Therefore, R_e is determined as an a.c. resistance between the working and auxiliary electrodes. In order to avoid the influence of E_a on the measurement of pH, the auxiliary electrode is connected to the detector electric circuitry via a capacitor which passes only the alternating component of the cell current.

Detector electronics

A schematic diagram of the detector electronics and its connection to the flow cell is illustrated in Fig. 2. The electronics are based on the simultaneous conductivity and amperometric detector described previously [20].

The conductivity channel is used without any change. Switch 5 enables the electronics to be switched from the amperometric to the potentiometric mode (e.g., pH measurement). The potential difference between E_w and E_r is measured by a voltage follower (9) based on a JFET input operational amplifier which accomplishes the current-free measurement. The capacities 3 and 4 are high enough for their a.c. impedances to be negligibly small in comparison with R_e at the frequency used

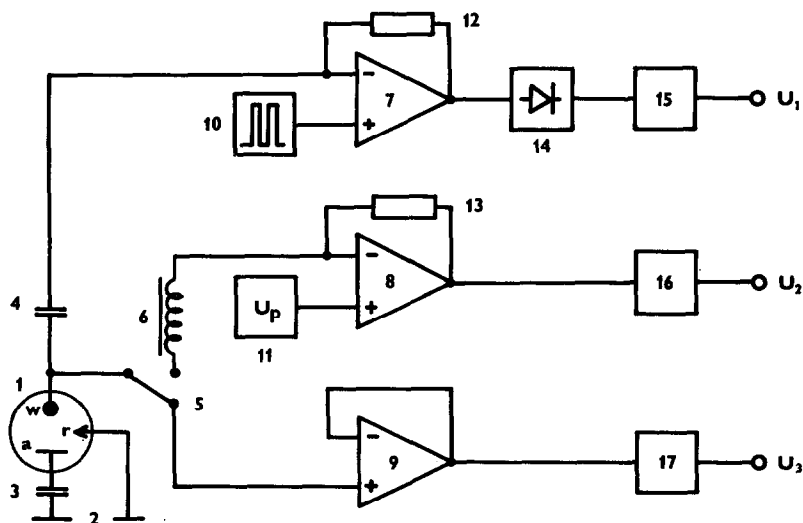


Fig. 2. Detector electric circuitry. 1 = Three-electrode flow cell; w, r and a = working, reference and auxiliary electrodes, respectively; 2 = common lead; 3, 4 = capacitors ($0.1 \mu\text{F}$); 5 = switch between amperometric and potentiometric detection mode; 6 = 7-H inductive coil; 7–9 = JFET input operational amplifiers; 10 = 1-V peak-to-peak, 17-kHz a.c. voltage source; 11 = d.c. polarizing voltage source; 12, 13 = feedback resistors; 14 = rectifier; 15–17 = circuitries for low-pass filtering, offset and gain control in each channel; U_1 , U_2 and U_3 = output voltages of conductivity, amperometric and potentiometric detection, respectively.

(17 kHz). The circuitries 15, 16 and 17 modify the output signals U_1 , U_2 and U_3 , respectively, by adjusting the offset, gain and cut-off frequency of low-pass filters to 2 Hz.

FIA arrangement

This consisted of an LD-2 syringe microfeeder (Development Workshops, Czechoslovak Academy of Sciences, Prague, Czechoslovakia), a laboratory-made six-port injection valve with a 50- μ l external loop and the flow cell described (Fig. 1A). The sampling loop was made of 500 \times 0.35 mm I.D. Teflon capillary tubing. The connection between the valve and the flow cell was made of 300 \times 0.2 mm I.D. Teflon capillary tubing. This capillary provided sufficient electrical insulation of the flow cell from the earthed sampling valve. The carrier fed by pump was a solution of tris(hydroxymethyl)aminomethane (Tris) sulphate (pH 8.2) and the conductivity $\kappa = 0.108 \text{ mS cm}^{-1}$.

Microcolumn liquid chromatograph

The chromatograph consisted of a MC 300 micropump (Mikrotechna, Prague, Czechoslovakia), a laboratory-made four-port injection valve with a 1- μ l internal sampling loop, a CGC 150 \times 1 mm I.D. microcolumn (Tessek, Prague, Czechoslovakia) packed with Separon SGX C₁₈ (5 μ m) and the detector described. The microcolumn output was connected to the detector by 100 \times 0.2 mm I.D. Teflon capillary tubing. The mobile phase was 1 mmol l⁻¹ tetrabutylammonium (TBA) hydroxide and 2 mmol l⁻¹ benzoic acid in deionized water, with pH 4.0 and $\kappa = 170 \mu\text{S cm}^{-1}$. The pH values of the prepared carrier, the mobile phase and sample solutions were measured with an OP 208/1 pH meter (Radelkis, Budapest, Hungary). The conductivity of solutions was measured with an OK 102/1 bath conductimeter (Radelkis). All measurements were carried out at laboratory temperature (25°C).

Chemicals

Morpholinoethanesulphonic acid (MES) and N-ethylmorpholine were supplied by Serva (Heidelberg, Germany). The alkyipyridinium salts were conveniently prepared from pyridine and the corresponding alkyl halides. Other chemicals were obtained from Lachema (Brno, Czechoslovakia). The deionized water used for the preparation of solutions had a conductivity $\kappa = 1.5 \mu\text{S cm}^{-1}$.

RESULTS AND DISCUSSION

The dynamic characteristics, linearity and mutual independence of output signals were studied using the FIA arrangement. The shape of the responses of both output voltages U_1 and U_3 after injection of 50- μ l pulses of the sample solution is shown in Fig. 3. On the abscissa, both volume and time units are given in order to show the change in the detector output voltages with both volume passed and time after the sample injection. Fig. 3 shows that after the front ascending edge, the state is reached where both signals do not change until the rear descending part of the injected pulse. Such a shape of the signal indicates that at the maximum deflection (*i.e.*, prior to the descending edge) the composition of the liquid passing through the detector corresponds to the composition of the sample injected. Such conditions make it

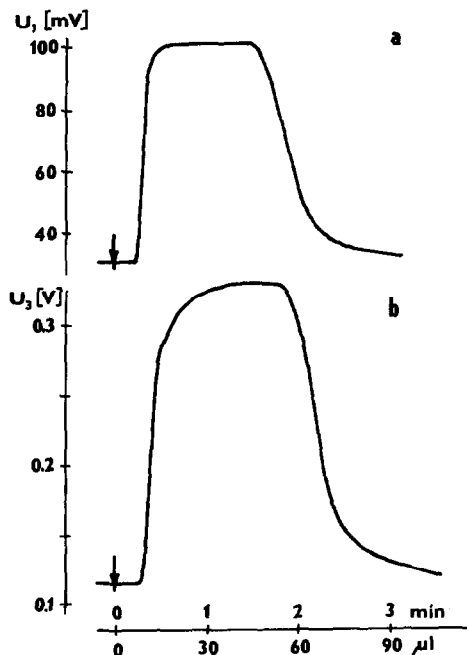


Fig. 3. Dependence of output voltages (a) U_1 and (b) U_3 on liquid volume passed through flow cell of the detector. Carrier: Tris sulphate, $\text{pH} = 8.2$, $\kappa = 108 \mu\text{S cm}^{-1}$; flow-rate, $0.5 \mu\text{l s}^{-1}$. Sample: $50 \mu\text{l}$ of sodium acetate, $\text{pH} = 4.2$, $\kappa = 1050 \mu\text{S cm}^{-1}$.

possible to obtain the dependence of output signals on the pH and conductivity of the solution in the cell by injecting a solution with known pH and conductivity.

In order to obtain this dependence, several solutions of inorganic and organic, anionic, cationic and amphoteric buffering compounds were injected. The compounds chosen were those often considered as mobile phase components in the liquid chromatography of ionic solutes. The pH and conductivity of the injected solutions were measured by the bath pH meter and conductimeter just before the injection. The dependences obtained are shown in Fig. 4.

The mutual independence of both output voltages, U_1 and U_3 , can be seen from following two sets of measurements which were included in Fig. 4. First, several solutions of sodium acetate (● in Fig. 4) with a constant pH (4.2 ± 0.05) and various conductivities were injected. The U_3 value obtained was constant and U_1 was a function of the conductivity of injected solution. Second, solutions of ethylenediamine phthalate (○ in Fig. 4) with a constant conductivity ($\kappa = 1.05 \pm 0.03 \text{ mS cm}^{-1}$) and various pH values were injected. The U_1 value obtained was constant whereas U_3 was dependent on the sample pH.

Further, several other salt solutions of known pH and conductivity were injected. The values of U_1 and U_3 obtained fall on a line common to all solutions with the exception of sodium lactate and sodium tartrate in the U_3 vs. pH dependence. These exceptions can be explained by complexing of the ions released from the working electrode by anions of these salts [17,21].

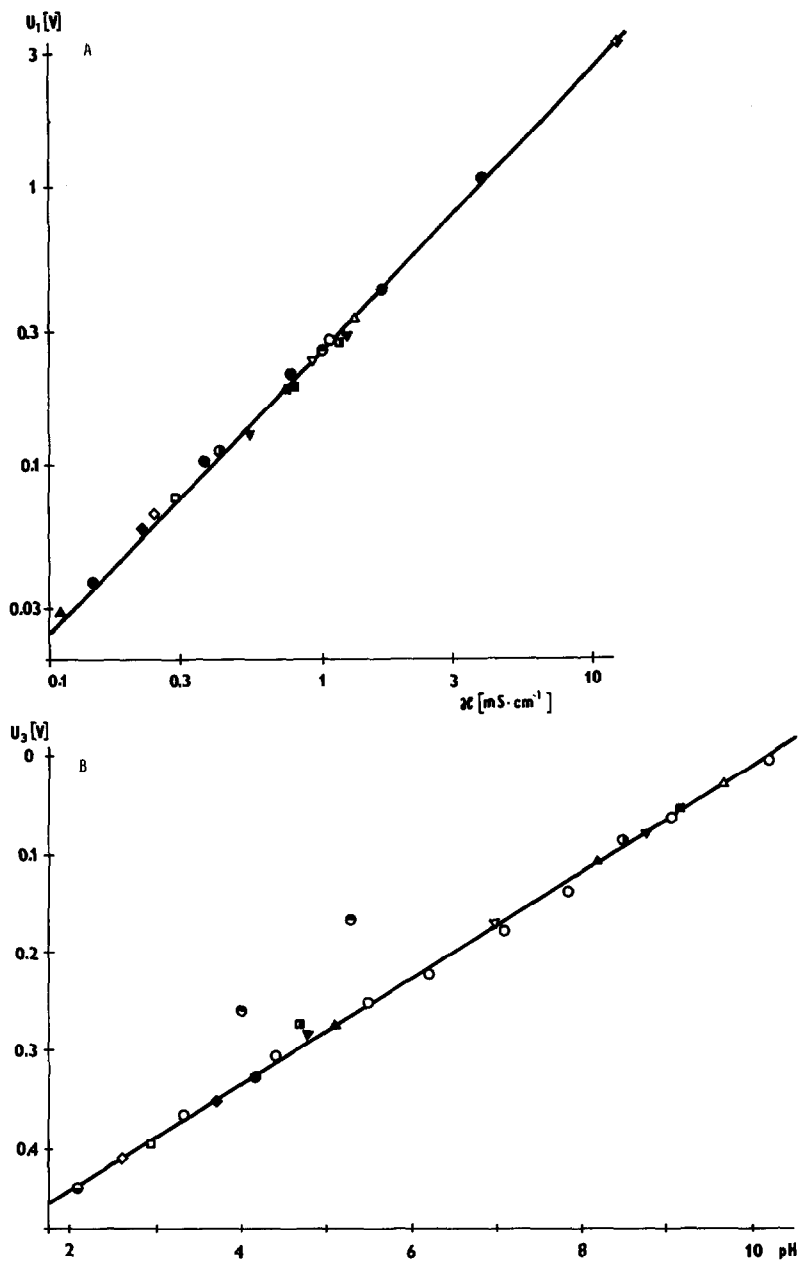


Fig. 4. Dependences of detector output voltages U_1 and U_3 on solution (A) conductivity and (B) pH. Solutions: ●, sodium acetate; ○, ethylenediamine phthalate; ⊙, phthalic acid; ⊖, sodium tartrate; ⊕, sodium hydrogencarbonate; ■, sodium tetraborate; □, nicotinic acid; ▣, sodium lactate; ▲, sodium morpholinoethanesulphonate; △, carrier [tris(hydroxymethyl)methylamine sulphate]; ▴, ammonium sulphate; ▼, potassium phosphate; ▽, ethylmorpholino sulphate; ◇, benzoic acid; ◆, β -alanine sulphate; ⋄, 0.1 M potassium chloride. For other conditions, see Fig. 3.

Using the least-squares method, the experimentally obtained points in Fig. 4A were fitted for the U_1 vs. conductivity curve with the equation U_1 (mV) = $a\kappa^b$ (κ in $\mu\text{S cm}^{-1}$). The values found, $a = 0.227$ and $b = 1.017$, indicate good linearity of the response. The points in Fig. 4B give the dependence of U_3 on pH according to the equation U_3 (mV) = $546 - 53.1\text{pH}$. The slope found is lower than the theoretical value (59 mV/pH), which can be explained by the purity of the working electrode material [17]. The value of U_3 calculated for pH = 0 corresponds approximately to the difference in half-cell potentials of the Pb/PbSO₄/3 mol l⁻¹ SO₄²⁻ electrode, $E_0 = -0.38$ V, and the Sb/Sb₂O₃ electrode at pH = 0, $E_0 = +0.15$ V [22].

The speed of response, *i.e.*, the speed of equilibration of the detector output signal to the value which corresponds to the actual composition within the flow cell, is the important parameter in LC. In order to obtain some information about this detector property, a solution of sodium acetate of pH 4.2 and $\kappa = 1.05$ mS cm⁻¹ was injected into the stream of carrier, Tris sulphate, of pH 8.2 and $\kappa = 0.108$ mS cm⁻¹ at different flow-rates. The front edges of the detector responses obtained are shown in Fig. 5.

The trace of U_1 can be considered to follow the actual profile of the conductivity change in the cell, as the small delay of the detector electronics (*ca.* 0.5 s) can be neglected even at the highest flow-rate (0.5 s corresponds to $0.25 \mu\text{l}$ at $0.5 \mu\text{l s}^{-1}$). The steepness of the edge depends on the flow-rate owing to the mixing in the capillary between the sampling valve and the detector cell. However, U_3 shows considerable delay when compared with U_1 . It should be noted that the two responses cannot be directly compared, as pH changes according to the degree of neutralization of mixed buffers, *i.e.*, considering the solutions used, the composition which corresponds to one

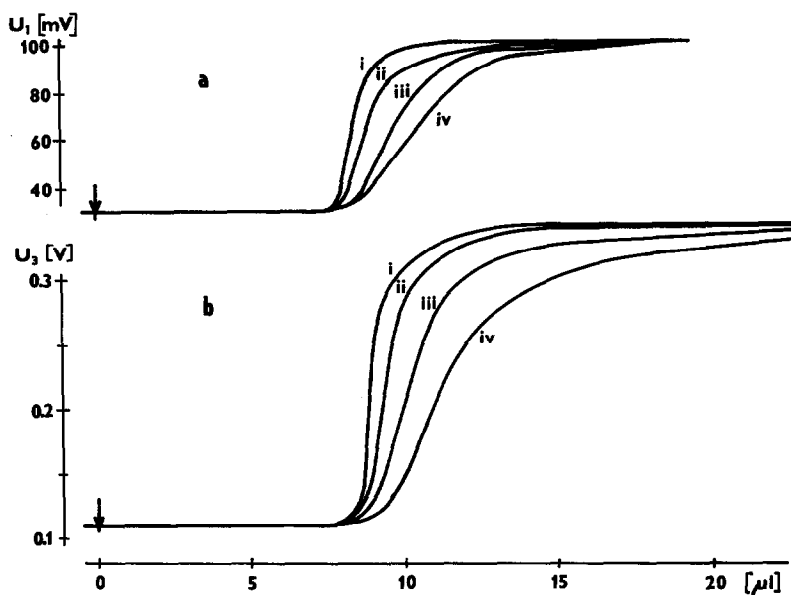


Fig. 5. Responses of output voltages (a) U_1 and (b) U_3 to step change in liquid composition at different flow rates: (i) 0.05; (ii) 0.1; (iii) 0.25; (iv) $0.5 \mu\text{l s}^{-1}$. For other conditions, see Fig. 3.

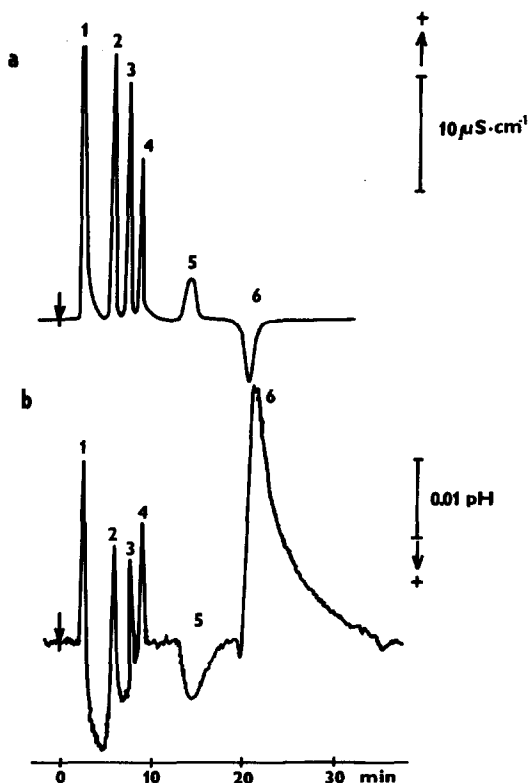


Fig. 6. Chromatograms obtained from (a) conductivity and (b) pH outputs of the detector. Column: CGC glass microcolumn (150 mm \times 1 mm I.D.) packed with Separon SGX C_{18} (5 μ m). Mobile phase: tetrabutylammonium hydroxide (1 mmol l⁻¹) and benzoic acid (2 mmol l⁻¹) in water, pH = 4.0, κ = 170 μ S cm⁻¹; flow-rate, 0.75 μ l s⁻¹. Sample volume, 1 μ l. Sample components and concentration (mmol l⁻¹): KNO₃ (2.5), KBr (4), *n*-hexylpyridinium chloride (4). Solute identification in the chromatograms: 1 = injection and K⁺; 2 = Cl⁻; 3 = Br⁻; 4 = NO₃⁻; 5 = *n*-hexylpyridinium; 6 = system peak.

quarter of the total increase in conductivity should give about three quarters of the total change in pH. However, such a pH value is actually reached only after a 7–10 s delay for all flow-rates used. Such a delay can only be ascribed to the slow surface response of the antimony working electrode [17].

Despite the delay found in the pH response, the simultaneous conductivity and pH detector can provide useful information about the separation of ionic compounds. Fig. 6 shows the chromatograms obtained by simultaneous monitoring of the output voltages U_1 and U_3 of the detector when used in the ion interaction chromatography of anions and cations [1,23]. In Fig. 6a and b, the directions of increasing conductivity and pH, respectively, are indicated by arrows.

The eluted peaks of inorganic anions, Cl⁻ with capacity factor $k' = 1.8$, Br⁻ with $k' = 2.7$ and NO₃⁻ with $k' = 3.4$, give rise to an increase in κ and a decrease in pH. The positive peaks on the conductivity trace are due to the higher equivalent conductivities of these anions when compared with benzoate anion in the mobile

phase. The decrease in pH can be explained by ion-exchange of anions of a weak acid (benzoate) for anions of strong acids [19]. Despite the delay in the pH trace of the detector, the peak width of anions 2, 3 and 4 in the pH diagram is comparable to that of the peaks in the conductivity diagram.

Peak 5 ($k' = 6.2$) corresponds to the elution of *n*-hexylpyridinium cation. The positive response in the conductivity detection mode results from an ion-exclusion retention mechanism of this organic cation. The increase in pH in its zone is due to the increase in ionization of benzoic acid in the mobile phase. Similarly, increases in κ and pH were also found in eluted zones of *n*-butylpyridinium ($k' = 0.6$) and *n*-pentylpyridinium ($k' = 1.8$) ions. Thus, the direction of the pH response is not a function of solute capacity factor, but depends on the sign of the solute charge.

Finally, the system peak 6 is negative on both the conductivity and pH outputs. Its remarkable feature is the narrow peak in the conductivity diagram and the very broad peak in the pH diagram. This peak width cannot be caused by slowness of the pH electrode. Very broad peaks of pH response were also obtained for some solutes when using electrochemical detection for monitoring electrochemically inactive ions [14,15]. The origin of such broad peaks must lie in pH equilibration within the column.

In the chromatographic arrangement, the noise of the conductivity signal was found to be 0.4 mV in U_1 which is equivalent to 25 nS cm^{-1} when using a mobile phase of conductivity $\kappa = 170 \text{ } \mu\text{S cm}^{-1}$. The noise of the pH output was equivalent to 0.002 pH unit and the drift was 0.004 pH unit within 20 min.

CONCLUSION

The detector described provides simultaneously independent conductimetric and potentiometric signals using a single flow cell of volume 150 nl. It can be used both in miniaturized FIA and microcolumn LC. The potentiometric detection mode was employed for the continuous monitoring of solution pH by an antimony working microelectrode. The potentiometric detection of other solutes would be possible when using working microelectrodes made of other materials, e.g., copper or silver.

The detector can be useful for monitoring internal gradients in microcolumn LC, especially gradients of pH and ionic strength. Despite the slower response to the solution pH, it can also provide useful information when detecting pH changes within the eluted solute zones. In this way, a deeper insight into the retention mechanism of the chromatography of ionic compounds may be obtained.

As the detector electronics are based on the previously described detector [20], it can alternatively be used in connection with an appropriate flow cell for simultaneous amperometric and conductivity detection, especially in micro-LC.

REFERENCES

- 1 J. G. Tarter (Editor), *Ion Chromatography (Chromatographic Science Series, Vol. 37)*, Marcel Dekker, New York, 1987.
- 2 W. Melander and Cs. Horváth, in M. T. W. Hearn (Editor), *Ion-Pair Chromatography (Chromatographic Science Series, Vol. 31)*, Marcel Dekker, New York, 1985, p. 27.
- 3 P. Jandera and J. Churáček, *Gradient Elution in Column Liquid Chromatography*, Elsevier, Amsterdam, 1985.
- 4 L. A. Æ. Sluyterman and O. Elgersma, *J. Chromatogr.*, 150 (1978) 17.

- 5 L. A. Æ. Sluyterman and J. Wijdenes, *J. Chromatogr.*, 150 (1978) 31.
- 6 J. P. Emond and M. Pač, *J. Chromatogr.*, 200 (1980) 57.
- 7 M. T. W. Hearn and D. J. Lyttle, *J. Chromatogr.*, 218 (1981) 483.
- 8 T. W. Hutchens, C. M. Li and P. K. Besch, *J. Chromatogr.*, 359 (1986) 157.
- 9 A. Hirose and D. Ishii, *J. Chromatogr.*, 387 (1987) 416.
- 10 A. Hirose and D. Ishii, *J. High Resolut. Chromatogr. Chromatogr. Commun.*, 10 (1987) 360.
- 11 C. Hongbo, E. Hansen and J. Růžička, *Anal. Chim. Acta*, 169 (1985) 209.
- 12 S. Egashira, *J. Chromatogr.*, 202 (1980) 37.
- 13 J. Georges and M. Khalil, *Anal. Chim. Acta*, 182 (1986) 281.
- 14 J. G. Tarter, *Anal. Chem.*, 56 (1984) 1264.
- 15 J. G. Tarter, *J. Liq. Chromatogr.*, 7 (1984) 1559.
- 16 B. Karlmark, *Anal. Biochem.*, 52 (1973) 69.
- 17 K. Schwabe, *pH Messtechnik*, Verlag Th. Steinkopf, Dresden, 3 Aufl., 1963, p. 86.
- 18 K. Šlais, *J. Chromatogr.*, 469 (1989) 223.
- 19 J. S. Fritz, D. T. Gjerde and Ch. Pohlandt, *Ion Chromatography*, Hüthig, Heidelberg, 1982.
- 20 K. Šlais, *J. Chromatogr.*, 436 (1988) 413.
- 21 J. T. Stock, W. C. Purdy and L. M. Garcia, *Chem. Rev.*, 58 (1958) 611.
- 22 R. C. Weast (Editor), *Handbook of Chemistry and Physics*, CRC Press, Boca Raton, FL, 68th ed., 1987, p. D-154.
- 23 J. Ståhlberg and A. Furungen, *Chromatographia*, 24 (1987) 783.